Identification of Blood Protein Biomarkers of Acute Liver Injury by Targeted Quantitative Proteomics in Acetaminophen and Carbon tetrachloride treated Mouse Models and Acetaminophen Overdose Patients

RUNNING TITLE: Blood biomarkers for drug-induced liver injury

Shizhen Qin[1], Yong Zhou[1], Li Gray[1], Ulrike Kusebauch[1,] Laurence McEvoy[3], Daniel J Antoine[3], Lucy Hampson[3], Kevin B Park[3], David Campbell[1], Juan Caballero[1], Gustavo Glusman[1], Xiaowei Yan[1], Taek-Kyun Kim[1], Yue Yuan[1], Kai Wang[1], Lee Rowen[1], Robert L Moritz[1], Gilbert S Omenn[1,2], Munir Pirmohamed [3]* and Leroy Hood[1]*

1. Institute for Systems Biology, USA
2. Departments of Computational Medicine & Bioinformatics, Internal Medicine, an Human Genetics and School of Public Health, University of Michigan, USA
3. Institute of Translational Medicine at University of Liverpool, England

*To whom correspondence should be addressed:

Dr. Leroy Hood, (MD, PhD, Professor, President) Institute for Systems Biology, 401 Terry N, Seattle WA, 98109-5234 USA; Email: Leroy.Hood@systemsbiology.org; Fax: 206 732 1299

Dr. Munir Pirmohamed (FRCP, PhD, Professor, Director), MRC Centre for Drug Safety Science, University of Liverpool, Block A: Waterhouse Building, 1-5 Brownlow Street, Liverpool L69 3GL; Email: munirp@liv.ac.uk; Fax +44 151 7945059

ABSTRACT:

Organ-enriched blood proteins, those produced primarily in one organ and secreted or exported to the blood, potentially afford a powerful and specific approach to assessing diseases in their cognate organs. In this paper, we demonstrate that quantification of organ-enriched proteins in the blood offers a new strategy to find biomarkers for diagnosis and assessment of drug-induced liver injury (and presumably the assessment of other liver diseases). We used selected reaction monitoring (SRM) mass spectrometry to quantify 81 liver-enriched proteins plus three aminotransferases (ALT1, AST1, and AST2) in plasma of C57BL/6J and NOD/ShiLtJ mice exposed to acetaminophen or carbon tetrachloride. Plasma concentrations of 49 liver-enriched proteins were perturbed significantly in response to liver injury induced by one or both toxins. We validated four of these toxin-responsive proteins (ALDOB, ASS1, BHMT and GLUD1) by Western blotting. By both assays, these four proteins constitute liver injury markers superior to currently employed markers such as ALT and AST. A similar approach was also successful in human serum where we had analyzed 66 liver-enriched proteins in acetaminophen overdose patients. Of these, 23 proteins were elevated in patients; 15 of 23 overlapped with the concentration-increased proteins in the mouse study. A combination of 5 human proteins, AGXT, ALDOB, CRP, FBP1, and MMP9, provides the best diagnostic performance to distinguish acetaminophen overdose patients from controls (sensitivity: 0.85, specificity: 0.84, accuracy: 85%). These five blood proteins are candidates for detecting acetaminophen-induced liver injury using next-generation diagnostic devices (e.g, microfluidic ELIZA assays).

KEYWORDS: liver-enriched proteins, selected reaction monitoring, drug-induced liver injury, acetaminophen, biomarker panel

INTRODUCTION

Adverse effects associated with therapeutic drugs are a serious health concern and a costly challenge for healthcare systems. Many drug-induced adverse effects target the liver due to their immediate exposure through first-pass pharmacokinetics and the liver's active roles in metabolizing xenobiotics. For example, overexposure to acetaminophen (N-acetyl-p-aminophenol, APAP), a widely used analgesic and antipyretic agent, is a leading cause of acute hepatic failure and the second most common reason for liver transplantation in the United States (1-3). To protect consumers from the risk of severe liver damage from APAP overdoses, the FDA recommended discontinuation of prescription drug products containing more than 325 mg of APAP (FDA Drugs_Drug Safety and Availability_20140114). Besides therapeutics, environmental toxins can also cause significant liver injury; for example, the use of the cleaning agent carbon tetrachloride (CCl_4) and many other halogenated alkanes has been severely restricted due to their liver toxicity.

To assess probable injury to an organ, it is important to monitor biologic materials that originate exclusively or primarily in that organ, in this case, liver-enriched proteins. A gene (and hence protein) is considered to be organ-enriched if its transcript abundance in that organ is >10-fold higher than the maximal values of gene expression in any other tissues assessed. For decades, cellular integrity indicators, such as levels of the transaminases, alanine aminotransferase (ALT, GPT) and aspartate aminotransferase (AST, GOT) in serum, have been used to reflect liver injury. However, use of these enzymes as surrogate markers of liver injury is not ideal. Since they are ubiquitously expressed at similar levels in multiple organs, an interpretation of their

change in levels in blood in response to a toxin can be complicated as a consequence of these enzymes originating from many tissues other than liver. For example, on the second day following a myocardial infarction, 98% of patients have higher levels of AST activity in blood (4). In addition to the fact that a particular enzyme may be heavily expressed in several different tissues, the existence of isozymes, often distributed differently among different tissues, may further complicate their measurements as, in laboratory tests, the combined activities of all isozymes are usually measured. Indeed, the *AST* protein is encoded in humans as two orthologous genes; *AST1* is highly expressed in heart, muscle, brain, liver and kidney, while *AST2* is more highly expressed in heart and skeletal muscle and a few other organs than in liver. Any injury to these tissues will cause elevated AST activity in the blood. ALT is more liver-enriched than AST, with an estimated two-fold higher transcript concentration in liver than in any other organ (Illumina Body Map). However, the distribution of two ALT isozymes, ALT1 and ALT2, is analogous to the AST isozymes with significant abundances represented across multiple organs, e.g., muscle, heart, liver and pancreas. Separating the two different forms of ALT is possible by isozyme-specific antibodies (5), but this test is not widely used in clinical laboratories. The short half-lives of circulating ALT (47 hours) and AST (17 hours) activities further limit their use in detecting drug-induced liver injury (6). Other enzymes such as alkaline phosphatase (ALP), gamma-glutamyl transpeptidase or transferase (GGT), KRT18 (keratin-18, full-length FL-K18, M65 and the caspase-cleaved fragment cK-K18, M30) and High Mobility Group Box-1 (HMGB1) have been reported as potential markers for APAP-induced liver injury (7, 8). However, none of these proteins is liver-enriched; accordingly, they do not specifically reflect hepatic injury.

In addition to protein markers, the levels of specific circulating RNAs such as the liver-enriched microRNA miR-122, and liver-specific transcripts, including those encoding albumin and transferrin, have been reported as blood biomarkers for reflecting liver injuries (9, 10). However, the clinical performance of these RNA-based blood biomarkers is yet to be determined.

Selected Reaction Monitoring (SRM), a targeted mass spectrometry-based proteomic approach that has molecular specificity and performs at high-sensitivity, is particularly powerful in quantifying a predetermined set of proteins in a complex mixture of proteins such as blood across a multitude of samples (11-13). We identified liver-enriched transcripts and then employed SRM analyses to determine which could be detected in blood. To identify more informative protein biomarkers that reflect liver injury, we adapted SRM to interrogate the levels of liver-enriched proteins in plasma collected from mice that have been exposed to APAP or CCl_4. This strategy was further tested in human serum as a means of identifying potential biomarkers to reflect liver injury from APAP-overdosed patients.

MATERIALS AND METHODS

Animals, drug treatment and plasma preparation

All work involving live animals was conducted under Institutional Animal Care and Use Committee (IACUC) approved protocols (10-00 series) with an assurance on file with the Office of Laboratory Animal Welfare (OLAW Assurance #A4355-01) and is accredited by the Association for Assessment and Accreditation of Laboratory Animal Care (AAALAC Accreditation #001363). All animal work was performed in our pathogen-free (SPF) vivarium

facility.

Female C57BL/6J (B6, stock number 000664) and NOD/ShiLtJ (NOD, stock number 001976) mice at 8 weeks of age were purchased from Jackson Laboratory (Bar Harbor, Maine). Animals were injected intraperitoneally (*ip*) with a single dose of 375 mg/kg of PBS-dissolved acetaminophen (BioXtra, ≥99.0% pure, Sigma Aldrich) or 1ml/kg of CCl_4 (anhydrous, ≥99.5% pure, Sigma-Aldrich) 1:10 (*v/v*) diluted in sterile corn oil. These doses were based on pathology examinations from pilot tests and are in similar dosage ranges with other studies (14-17). Vehicle groups received the same volume of PBS (APAP) or corn oil (CCl_4). No-treatment controls for each mouse strain were included. In the APAP model system, mice were fasted for 24 hours before injection. The detailed procedures are summarized in Supplementary Table 1. Plasma was collected and prepared following Tammen's protocol (18). Briefly, blood samples were centrifuged at 1,300 X g for 10 minutes at room temperature followed by a second centrifugation of the supernatant at 2,500 X g for 15 minutes. Plasma samples were stored at -80°C without proteinase inhibitors. Livers from sacrificed animals were excised and stored at -80°C with a section of each liver preserved in 10% buffered formalin for H&E staining.

Liver injury assessment in APAP and CCl_4 mouse models

The degree of liver injury in mice was assessed by ALT and AST enzyme activities (19, 20) and histology H&E staining (detailed procedures in Supplementary Materials).

Plasma acetaminophen concentration measurement

Plasma APAP concentrations in mice were measured with an acetaminophen ELISA kit that

shows less than 2% cross reactivity toward similar compounds such as procainamide (Neogen Corporation, Lexington, KY). Because it is a competitive ELISA assay, the extent of color development is inversely proportional to the concentration of APAP in samples that were determined with a standard curve.

Liver total glutathione and GSH/GSSG ratio in mice after fasting

Total liver glutathione and GSH/GSSG ratios were measured with GSH/GSSG-Glo assay, a luminescence-based system for the detection and quantification of total glutathione (GSH +GSSG) and GSH/GSSG ratios (Promega, Madison, WI). Five female NOD mice, 8 weeks of age, were fasted for 24 hours similarly to the APAP-treated group described. Liver samples were collected at the end of fasting, tissue lysates prepared and tested following the manufacturer's instructions.

Human APAP overdose patient samples

We conducted a prospective study where patients admitted to the Royal Liverpool University Hospital (UK) with acetaminophen overdose were recruited after providing written informed consent. The study was approved by the Liverpool Local Research Ethics Committee. Patients presented at various times after their overdose and had taken differing amounts of acetaminophen. According to treatment guidelines in the UK, these patients were treated with N-acetylcysteine (NAC) if the acetaminophen levels were above the treatment threshold lines. Some patients presented with a staggered overdose (ingestion of multiple doses of APAP over a period of >1 hour), and, as per guidelines, they were treated irrespective of serum acetaminophen levels. In every case, a first blood sample was drawn and ALT level tests were performed before

NAC treatment. The ALT levels (reference range females <35 IU/L, males <40 IU/L) recorded in the patients varied according to the amount of acetaminophen taken and the time of presentation after the overdose. Detailed information on the 14 patients studied is summarized in Supplementary Table 2. We also analysed control serum samples taken from healthy volunteers who had not consumed any acetaminophen for at least 2 weeks prior to recruitment.

Human and mouse sample preparation for SRM

To reduce the protein complexity, fourteen highly abundant blood proteins (HAP) were depleted from each plasma or serum sample using an AKTA FPLC (fast protein liquid chromatography) system (GE Healthcare, USA) coupled with a custom-ordered mouse IgY14 LC5 column or a human IgY14 LC2 depletion column (Sigma-Aldrich, USA), respectively. All control and treated samples were processed similarly with about 90% of the total protein depleted from mouse, or 95% removed from human samples. Depleted samples were digested with trypsin and desalted with Oasis MCX cartridges (Waters, Milford, MA) as previously described (21).

Preparation of liver tissue samples for SRM analysis

Mouse liver tissues kept at -80 C° were lysed and homogenized in lysis buffer (1:10 g/ml) (0.1% SDS in 100 mM sodium phosphate buffer, pH7.5 with protease inhibitor cocktail from Sigma/Pierce) in a PreCellys homogenizer at speed of 6,500 rpm for 3 X 45 seconds in a cold room. The homogenizing program was repeated once. Supernatant fraction was collected after spinning for 10 min at 14,000 X g at 4°C. Extracted liver proteins in the supernatant were digested with trypsin and desalted with MCX cartridge.

Mass spectrometry

All SRM analyses were performed on the Agilent 6460 (mouse) and 6490 (human, replaced 6460 after mouse study) triple quadrupole (QQQ) mass spectrometers. Both mass spectrometers were equipped with a ChipCube nano-HPLC device. An Agilent HPLC chip (Cat # G4240-62101, large capacity 160 nL trap, 150 mm C18 column) was used for peptide separation. Spray voltage was set at 1800 V. A 2µg sample aliquot of depleted serum, plasma or liver lysate was loaded and eluted over a 60-minute gradient with 0.66% per minute acetonitrile slope in the presence of 0.1% formic acid. Peptides were analyzed in dynamic SRM mode with 4-15 minutes retention time window according to number of concurrent transitions. The cycle time was set at 2500 ms.

Building the mouse and human liver-enriched protein list

Liver-enriched proteins for mouse and human were generated respectively with multiple microarray and RNA-Seq body-map datasets, including BioGPS, NCBI/GEO, Illumina Body Map and in-house ISB human-tissue atlas (Supplemental Materials). From the liver-enriched transcripts, we identified the candidate blood liver-enriched proteins that could be quantified with SRM mass spectrometry.

SRM method generation and optimization

As described previously (21), target peptides and transitions were selected to ensure they are proteotypic (specific) to the protein of interest. ISB in-house proteomics databases, e.g., PeptideAtlas for mouse (22) and SRMAtlas for human (23), were used to facilitate this process.

Of all the peptides (about 130 for each species) we only have 6 peptides that are common for the same protein between human and mouse. A three-step optimization procedure was conducted to identify the best-performing 2 peptides for each protein and top 4 transitions for each peptide (Supplemental Materials). The numbers of proteins and peptides in each step are summarized in Supplementary Table 3. Final SRM methods applied for the 52 mouse and 66 human proteins are summarized in Supplementary Table 4 sheet 1 (human) and sheet 2 (mouse)

Crude unpurified peptide standards were synthesized with heavy isotopic lysine ($^{13}C_6{}^{15}N_2$) or arginine ($^{13}C_6{}^{15}N_4$) at the C-termini (heavy PEPscreen® peptides, Sigma-Aldrich, St. Louis, MO, USA). SRM conditions including collision energy (CE, vendor-provided default formula *CE=0.036*m/z − 4.8* for 6460 and *CE=0.036*m/z – 7.3* for 6490) were optimized with heavy labeled synthetic peptides and titration curves were generated for each peptide. The proper spike-in amount of heavy peptides was determined to reach an L/H ratio within ± 10 fold in most samples. Characterization of titration curves of the heavy peptide standards from the 5 best classifier proteins in the human APAP overdose study is shown in Supplementary Figure 1.

SRM samples and data analysis and statistics

In the mouse study, two mice (#1 and #2) were analyzed for each time point, except for the 8h and 24h time points in the APAP model, in which 3-4 mice were monitored. In the human study, all 12 healthy volunteer and 14 patient samples were analyzed. Duplicate mass spectrometry runs were performed for each sample.

SRM data were processed using the Skyline targeted proteomics environment (24). The total peak area and Light/Heavy (L/H) ratio of each peptide were exported and normalized to the

original blood volume. An algorithm similar to that used in a proteomic characterization of pulmonary nodules study (25) was developed to evaluate how well each protein was able to predict liver toxicity induced by APAP or CCl_4 and to identify the best classifiers. Classification performance of protein panels was estimated with support vector machine (SVM). Using the LibSVM package built in the Waikato Environment for Knowledge Acquisition (WEKA) version 3.6.11, a non-linear SVM classifier with radial basis kernel function was constructed. WEKA's default settings were used for all parameters including a hyperparameter and a marginal value. To compute the classification accuracy and probability estimates, a 10-fold cross validation approach was performed. Based on the probability estimates, ROC (Receiver Operating Characteristic) curve and the area under the curve (AUC) were generated with the MedCalc toolbox in Matlab. All other analyses, including *t*-test and all graphics, were generated by Microsoft Excel, MultiExperiment Viewer (MeV) (26) or Prism 5 (GraphPad Software, La Jolla, CA, USA).

Western blotting

Aliquots of 0.5µl serum or plasma (not depleted) from human or mice samples were loaded on 4-12% SDS-PAGE Bis-Tris gels (Life Technologies, Grand Island, NY USA). Following separation, the proteins were transferred to PVDF membrane using an iBlot® dry blotting system from Life Technologies and probed overnight at 4ºC with primary antibodies. After washing with TBS-T (0.1% Tween 20 in TBS), membranes were incubated with HRP-conjugated secondary antibodies for 1 hour at room temperature. Detection was carried out by enhanced chemiluminescence (Thermo Scientific, Rockford, IL) with a CCD camera (ProteinSimple, Santa Clara, CA). The images were analyzed using ImageJ. Commercial antibodies were ordered from

Protein Tech group (ALT1, AST1, AST2, ASS1, BHMT, CRP and GLUD1, Chicago, IL), Epitomics (ALDOB, Burlingame, CA), ABNOVA (FBP1, Taipei, Taiwan) and Cell Signaling (MMP9, Danvers, MA), respectively.

RESULTS

Significant drug-response variations were seen in APAP-treated but not in CCl_4-treated mice

Liver injury in mice induced by a single *i.p*. injection of hepatotoxins APAP or CCl_4 was initially assessed by ALT and AST enzyme activities in plasma, and later confirmed by histological examination. In APAP-treated mice, the plasma ALT and AST activities peaked 8 to 24 hours post-treatment in NOD and 24 to 48 hours for B6 mice, respectively. In CCl_4 exposed mice, the peak times were slightly delayed compared with APAP - 24 hours for NOD and 48 hours for B6 mice, respectively. In the CCl_4-exposed mouse model, the toxin-responsive variations measured by ALT and AST activities were small among mice in both strains; however, significant variations were observed in the APAP-treated groups. For example, at the peak time point (8h), a greater than 80-fold difference in ALT activity was observed between hyper-responsive (mouse 8h2 – mouse #2 at 8 hour) and hypo-responsive (8h1) NOD mice. Similar results were observed among APAP-treated B6 mice. In all cases, the levels of ALT and AST levels were parallel to each other (Figure 1A). Histopathological examination (H&E staining) showed typical toxin-responsive zone III centrilobular necrosis as described by Davidson (27) and Boyd (28) in animals from the APAP and CCl_4-treated groups; the severity of liver injury based on

histopathology analysis agrees with the relative changes ALT and AST activities measured in plasma (Figure 1B and 1C).

Plasma APAP concentrations are similar in mice with different degrees of toxic responses

Blood APAP concentrations and ALT activities were measured in five NOD and five B6 mice at 3h and 8h time points. In both NOD and B6 mice, APAP can be detected in plasma 3 hours after drug administration. In all 5 animals tested in both strains, similar APAP levels were observed regardless of their difference in blood ALT activities in both strains. For example, APAP levels in NOD mice range from 89 to 111 μg/mL while ALT activity ranges from 54 to 212 IU/L; similarly, APAP levels in B6 mice range from 33 to 52 μg/mL while ALT activity ranges from 102 to 1242 IU/L from the hypo-responder to the hyper-responder. There was no positive correlation between plasma APAP concentration and ALT activity in the blood (Supplementary Table 5). At 8 hours post injection, plasma APAP concentrations in all tested animals fell back to zero in both strains.

Liver total glutathione content and GSH/GSSG ratios are similar after fasting in mice

Another possible explanation for the individual differences in response to APAP treatment is the liver level of dithiolthiones, specifically glutathione (GSH), a key detoxification compound that neutralizes toxic APAP or CCl_4 metabolites in the liver (29, 30). The levels of GSH and the ratios of GSH/GSSG (oxidized form of GSH) were measured in five NOD mice livers at 24 hours after fasting. No significant inter-individual differences were observed in either total glutathione levels (from 4.90 to 5.79 nmole/mg liver, relative standard deviation RSD =6.8%) or GSH/GSSG ratios (from 45.4 to 49.8, RSD=3.4%) among the 5 mice (Supplementary Table 6).

Forty-nine informative proteins distinguish APAP or CCl_4-treated mice from controls

Responses to APAP and CCl_4 in both B6 and NOD strains were similar except that the NOD strain was more responsive to both hepatotoxins as evidenced by earlier response time and higher ALT and AST enzyme activities compared to baseline values. Therefore, subsequent work, *i.e.*, SRM proteomics and Western Blotting, focused on the NOD strain. Of the 52 proteins successfully measured in both APAP and CCl_4 treated mice, we identified 49 informative proteins (including known liver toxicity markers AST and ALT which are not liver-enriched) with plasma levels reproducibly changed in response to APAP or CCl_4 induced liver injuries. Of these, 25 (including AST and ALT) showed concentration increases and 22 demonstrated concentration decreases in plasma after either APAP (responsive animals) or CCl_4 treatment. In APAP-treated animals, two protease inhibitor components, inter-alpha-trypsin inhibitor heavy chain 2 and 3 (ITIH2 and ITIH3), showed decreased plasma concentrations at pre- or peak response time (ITIH2, 3 and 8h time points, p=0.0002; ITIH3, 3, 8, 24h time points, p=0.0008). However, no concentration decreases were observed in CCl_4 treated mice at pre- or peak response time points (3 to 48h). Accordingly these two proteins may permit one to distinguish liver toxicities due to APAP exposure from those arising from CCl_4 exposure. Liver tissue SRM results were also compared (Table 1). The other liver-enriched proteins were not affected by drug treatment.

Plasma ALT and AST enzyme activities after APAP treatment paralleled each other with a Pearson's correlation coefficient of 0.97. When plotted against ALT enzyme activities, most of the 25 proteins with increased plasma concentrations measured by SRM correlated with ALT (thick black line) and AST (thick red line) activities (correlation coefficient r = 0.50 - 0.98, average 0.83) (Figure 2). Some proteins with lower r values did not correlate as well with ALT

enzyme activity after APAP insult. For example, plasma concentrations of GLUD1 in hyper-responders remained elevated up to 96 hours (183X control average) post APAP treatment when ALT enzyme activities dropped back to baseline level. Its prolonged elevation implies that GLUD1 may better reflect APAP-induced liver injury than ALT or AST activities due to the fact that the hepatopathology induced by APAP exposure remains 96 hours after treatment. In addition to GLUD1, other proteins with low r values may potentially serve as better markers than ALT or AST for early detection (Figure 2A). Similar results were observed in CCl_4 treated NOD mice with Pearson correlation coefficient ranging from 0.66 to 0.95 and an average of 0.86 (Figure 2B). In both APAP and CCl_4 NOD mouse models, the plasma levels of 12 proteins (AGXT, ALDOB, ASS1, BHMT1, DPYS, FAH, GLUD1, GNMT, IDH1, MAT1A1, MDH1 and UBP1) proved to be better indicators (in terms of fold change) than ALT or AST, for early (3 and/or 8 hours) and extended detection (72 and/or 96 hours) of APAP- and CCl_4- induced liver injury.

Validation by Western Blotting

To validate proteins that showed better performance than ALT or AST in reflecting the status of drug-induced liver injury, especially at early (3 and/or 8 hours) or late (72 and/or 96 hours) time points, we tested a number of antibodies specific for some of the liver-enriched proteins in Western blotting. Only antibodies against BHMT1, ALDOB, ASS1, and GLUD1 worked well in mouse plasma samples. All these proteins showed good correlations between the Western blot and SRM measurements. For example, in APAP treated NOD mice, despite clear microvesicular injuries indicated by histopathological examination at 3 hours post acetaminophen exposure, elevation of ALT and AST activities in plasma were not reliably detected. However, at the same time point ALDOB, ASS1 and BHMT were significantly elevated and detected clearly by SRM

as well as by Western blot. Differences in the levels of GLUD1, ASS1 and BHMT could also be readily detected at 96 hours post exposure when the ALT and AST levels declined rapidly to the normal range. GLUD1 in plasma could be detected as late as 144 hours post treatment by WB (Table 2A). Similarly, at 3 hours post CCl_4 treatment, while the ALT level increased slightly (76 IU/L, a 1.8 fold change over control average) and AST level showed no change. However, histopathology showed centrilobular microvesicular changes in the liver and meanwhile, plasma BHMT protein elevated from undetectable to a 40-fold increase over background level measured by SRM and later confirmed by Western blotting. The CCl_4 induced injuries extended beyond 144 hours based on our histopathology observations. Accordingly, elevations of ASS1 and GLUD1 protein were still reliably detected at 144 hours by Western analyses, whereas ALT and AST activities were only detectable at the 24-hour time point post exposure (Table 2B).

Identifying serum biomarkers to reflect liver injury associated with APAP overdose in human patients by SRM

To explore the possibility of using a similar approach to discover more effective serum biomarkers for liver toxicity, we monitored 66 liver-enriched proteins by SRM in sera from 14 APAP overdose patients and 12 controls. The 66 proteins are represented by 124 proteotypic peptides. We identified 23 proteins, including ALT and AST, with elevated levels (3 fold or higher) in APAP overdosed patients (Supplementary Table 7), over a wide range of times from the point of acute overdose. Five patients, LIV003, LIV004, LIV007, LIV013 and LIV014 were identified with higher than normal (female > 35IU/L, male > 40IU/L) ALT enzyme activity in serum. AST enzyme activities were not tested in patients. The results from SRM-based measurement showed only 3 of the 14 APAP overdose patients, LIV004, LIV013 and LIV014,

had higher than normal levels of ALT, AST1 and AST2. These differences of detection sensitivities on ALT and ASTs may be explained by the fact that ALT enzyme activities were analyzed on the same day samples were collected while SRM tests were performed 1 to 3 years later. Also, we defined a 3-fold increase as significant in the SRM tests.

For the remaining 43 proteins, no significant changes were observed in patients compared with controls, although 22 mouse orthologous proteins showed decreased plasma concentrations in APAP mouse model (Table 1).

The elevation of 23 proteins was observed in 12 of the 14 APAP overdose patients (except for patients LIV005 and LIV010) while ALT and AST protein levels were up only in 3 patients (patients LIV004, LIV013 and LIV014) by SRM (Supplementary Table 7). Multivariate statistical analysis revealed 5 human proteins: AGXT, ALODB, CRP, FBP1 and MMP9, that constituted a classifier panel that separated APAP overdose patients from healthy volunteers (Figure 3A) with an area under curve (AUC) of 0.84 (sensitivity 0.85, specificity 0.84 and accuracy 85%). For comparison, a combination of the two known liver markers ALT1 and AST1 reached an AUC of 0.46 (sensitivity 0.54, specificity 0.50 and accuracy 54%), adding ALT and AST to the 5-protein panel did not improve its diagnostic performance (Figure 3B). We tested the 7 aforementioned mouse antibodies and found antibodies against ALDOB and CRP worked well on human sera. Results showed good consistency between the SRM measurements and WB images (Figure 3C).

DISCUSSION

Finding blood biomarkers to reflect the status of specific pathological conditions has been a major focus in academia and industry. Various high throughput approaches have been applied to gain comprehensive molecular profiles, although there have been few successes translating the findings to clinically useful biomarkers (31). In developing diagnostic markers, the most common scheme is first to create a candidate panel by discovering molecules relevant to disease condition, assess the panel's diagnostic performance, and then validate the panel on a different set of samples (31). In order to discover markers that represent biological networks and hence could be employed as proxies for toxin-perturbed changes in their cognate networks in a particular organ, we employed a different strategy by focusing on proteins enriched in disease-associated organs. We identified 131 liver-enriched proteins for mouse by comparative organ-riched transcript analyses, then determined which of the proteins encoded by these transcripts could be detected in the blood and finally measured the concentration changes of these proteins by SRM in plasma samples from toxin-exposed mice. The same strategy was also used in serum samples from acetaminophen overdose patients.

Based on blood aminotransferase activity and histopathology examination, we observed inter-strain as well as inter-individual variations within the same strain in response to APAP treatment. Inter-strain variation in response to APAP is well documented, for example Harrill and colleagues reported a greater than 20-fold serum ALT concentration difference at 24 hour post drug administration amongst different mouse strains. In addition, the authors demonstrated that genetic variation in the gene orthologous to CD44 in human is associated with susceptibility to acetaminophen toxicity in two independent cohorts (32). In this study, we observed both inter- and intra- strain variations among NOD and B6 mice in response to APAP treatment that cannot

be explained by genetic heterogeneity. Even though not specifically discussed, data from some prior reports showed similar or greater inter-individual variations in ALT or AST activities in the mouse strain tested (32-34). Based on the similar blood APAP levels and glutathione reduced/oxidized state (GSH/GSSG) ratios in the livers from hypo-responsive and hyper-responsive individuals, we conclude that the observed inter-individual variation is not due to drug administration errors or differences in the glutathione content in liver, a key detoxification compound. Also, our study showed that female mice displayed similar degree of inter-individual variation as male mice in prior APAP toxicity studies. Thus, we can exclude the possibility of female specific biological features such as the menstrual cycle that may contribute to the difference in APAP response. Unlike APAP, our data indicated no significant inter-individual variation towards CCl_4 induced liver injury even though CCl_4 is also metabolized by P450 (35) and a GSH-dependent detoxification mechanism may protect the microsomal membrane against free-radical injury induced by this chemical (36). All these observations suggest that additional factors may contribute to the inter-individual differences in response to APAP exposure. For example, Claton *et al.* found an association between an individual's pre-dose urinary microbial metabolites p-cresol sulfate (PCS) and phenylacetylglutamine (PAG) concentrations, and the post-dose urinary acetaminophen concentration (37). Conversion of p-cresol to PCS is analogous to the conversion of acetaminophen to non-toxic acetaminophen sulfate. A person's capacity for acetaminophen sulfonation can be significantly reduced by competitive p-cresol sulfonation. Thus, an individual's spectrum of gut microbiota may trigger an adverse effect of a drug.

In the human study presented here, using a limited number of subjects with different confounding factors including ages, gender, weight, time of overdose, alcohol consumption,

eating disorders, hepatic disease, smoking and drug use history, we did not observe correlation between the patients' blood APAP concentrations and ALT levels (Pearson's correlation coefficient r-value 0.36; p-value 0.21, Supplementary Table 2). This is not surprising given the very different time points at which patients presented after APAP overdose.

Blood protein measurement results from this study demonstrated an excellent agreement of concentration-increase proteins in both mouse models and human APAP overdose patients. There are 15 concentration-increase proteins in the human APAP overdose study that overlap with proteins in the APAP treated mouse study. 14 of the 15 proteins (except APOA1) agree with each other with elevated protein levels after APAP exposure (Table 3). Some of the biomarker candidates identified in the mouse study have been reported. For example, in a glycocapture-assisted global quantitative proteomics (gagQP) study, we discovered 235 proteins that showed concentration changes at 48h after APAP exposure. Among them, 17 of the 135 proteins were liver-enriched proteins (38). Fourteen of those 17 liver-enriched proteins overlapped with the proteins identified in this study. The increase of hepatic MMP9 expression after CCl_4 exposure has been reported (39). In this study, we have shown that MMP9 levels increased in serum by up to 10-fold in four of the APAP overdose patients tested. ALDOB, one of the proteins increased in both hepatotoxin mouse models and in APAP-overdose patients observed in this study, has been reported with a dose-dependent concentration change in 95% of the patients with liver cell necrosis (40). GLUD1 is located in mitochondria and has been used as a marker for mitochondrial damage (41). Similar to our finding, increased GLUD1 activity in plasma has been reported in APAP overdose patients with abnormal liver function tests (LFT) (42). It is known that liver failure impairs CRP production by the liver (43), we demonstrated that serum CRP concentration increased up to 14-fold in APAP overdose patients

(Supplementary Table 7). CRP and MMP9 identified patients in this study that were otherwise indistinguishable from controls by the traditional liver injury markers ALT and AST. It has been reported that the increase of ASS concentrations in plasma is more sensitive than ALT; ASS levels appeared to increase early in some patients with APAP overdose, then decreased quickly in plasma after 24 hours of APAP exposure (44). Our mouse study showed a persistent increase of ASS1 concentration in plasma till 96 hours. Unfortunately, ASS1 was not detected in human serum samples by SRM or WB in this study.

Gene ontology enrichment analysis for biological process, cellular components and signaling pathways were performed with the 58 blood biomarker candidates identified which include 36 elevated (from both mouse and human studies) and 22 decreased their blood concentration (mouse study) after acute liver injury. A number of metabolic processes (biological networks) including steroid, glycosaminoglycan and amino acids metabolism, as well as glycolysis and lipogenesis are associated with these putative blood biomarkers for acute liver injury (Figure 4). These reflect major biological processes carried out in the liver and it is not surprising to see them change during acute liver injury.

All extracellular proteins exhibited decreased concentrations in mice plasma after APAP or CCl_4 exposure. Under normal conditions, these extracellular proteins are synthesized in hepatocytes and released into blood as part of normal hepatocyte functions. It is not surprising to see a decrease of these proteins in blood since the production and release of these extracellular proteins were impaired during liver injury. This concentration-decrease phenomenon after APAP treatment was not observed in humans. This may be due to the relatively high concentration of APAP administrated in the animal model system as compared to what the

human patients ingested. For examples, 375mg/kg of APAP was used in the mouse study which would translate to greater than 80 Tylenol tablets containing 325 mg acetaminophen per tablet taken by an average person. Massive damages in the livers were observed in mice at peak hours (Figure 1) and production of proteins that were normally secreted into the blood stream must be severally obstructed (resulting in decreased concentrations in serum). Since much lower APAP doses were taken by the overdosed patients, the liver damage probably was less severe in patients compared to mice and the hampered secretion of those liver proteins may be compensated by increased production in part of the liver that were not severely damaged.

It is interesting to note that most of the 36 proteins with increased plasma concentrations after APAP or CCl_4 exposure are intracellular (A1BG, CRP are 2 exceptions) and are involved in functions localized in hepatic zone 3—the zone that responds acutely to the two liver toxins used in the study. The hepatocytes in zone 3 have the poorest oxygenation and predominantly perform oxygen-independent metabolic processes, e.g., glycolysis and lipogenesis. In addition, some amino acid metabolism enzymes in the arginine, proline, alanine, aspartate, methionine and glutamate metabolism networks are also located in zone 3 (45). In this study, the blood concentration of two catalytic enzymes involved in glycolysis, FBP1 and ALDOB, were increased after APAP or CCl_4 exposure. In addition, AGXT, ALT, ASL, ASS1, AST, CPS1, and GLUD1 are involved in the citrate and urea pathways, which are connected with the glycolysis pathway. It is well known that threonine can be converted to glycine, then serine and later pyruvate. Enzymes involved in glycine, serine and threonine metabolic process including BHMT1, BHMT2, FAH, GNMT, HGD, HPD and SARDH, were increased in plasma after APAP or CCl_4 exposure. Some other cytosolic proteins (ADH1A, ADH4, ALDH1A1, ASL, ASS1, CPS1, DPYS and UPB1) are also either directly or indirectly involved in the metabolic

processes in zone 3. Five proteins with increased blood concentrations after APAP and CCl_4 treatment including ADH1A1, ADH4, ALDH1A1, CAT and HMGCS2 are annotated with process of response to oxidative stress and xenobiotic metabolism. MAT1A, GNMT and BHMT are mainly expressed in liver and are involved in methionine metabolism. MAT1A catalyzes the formation of biological methyl donor S−Adenosyl Methionine (SAMe) and GNMT is involved in regulating hepatic SAMe concentrations. There is evidence indicating the importance of labile methyl group in maintaining normal liver function (46). SAMe also plays a central role in epigenetic processes (47). It is well known that DNA methylation as an epigenetic factor influences drug metabolism (48). Interestingly, these enzymes may also affect liver regeneration that is critical after massive liver damages caused by toxins. For example, mice lacking MAT1A have reduced hepatic SAMe level which resulted in impaired liver regeneration (49).

It is well known that the liver is the main source of both coagulation factors and proteins involved in fibrinolysis. In the coagulation cascade, F10 activates thrombin (F2), which then cleaves FGA/FGB/FGG (fibrinogen, depletion target of IgY14 column, therefore was not tested in this study) and releases fibrins that polymerize to form blood clots. On the other hand, cleaved PLG (plasminogen) forms plasmin that degrades the fibrin clots (fibrinolysis). In acute liver injury, both clot formation and fibrinolysis are impaired. For example, the concentrations of PLG and SERPINF2 in fibrinolysis and F10, F2 and FGG in the fibrin formation were all decreased in blood after liver damage (Figure 4). This may explain why patients with liver diseases are often in hemostatic balance as a result of concomitant changes in both pro- and anti-hemostatic networks and this rebalanced hemostatic system is reflected clinically by the large proportion of

patients with liver disease who can undergo major surgery without any requirement for blood product infusion (50).

In addition to blood, the concentration of 49 proteins was also investigated by SRM in liver tissues. However, up- and down-regulations of protein expression in response to drug exposure was overshadowed by massive liver damages caused by the relatively high doses of APAP and CCl_4 as demonstrated by the fact that almost all the proteins tested showed decreased levels in liver tissue after drug exposure. This was in agreement with the observation that intracellular proteins increased their concentrations in blood due to cell lysis and extracellular proteins decreased their blood concentrations due to diminished normal production and secretion by liver cells after massive liver damage occurred.

Only two proteins of all those tested may have the ability to distinguish between injuries caused by APAP and CCl_4. (Table 1). This is consistent with the findings that both APAP and CCl_4 induce toxicities through similar metabolic processes with similar histopathological changes in the centrilobular area of the liver (51). This observation is also in agreement with the findings of Aleksunes et al. who showed that hepatotoxic doses of APAP and CCl_4 increased Ho-1, Nqo1 and Mrp4, and reduced Oatp1a1, 1a4, and Ntcp transcripts in liver in a similar pattern (52). The major difference between APAP and CCl_4 induced liver injury we observed was the peak response time determined by histopathology and plasma aminotransferase activities in mice: 8 hours post-exposure for APAP vs. 24 hours for CCl_4. This delayed response may be due to the compound vehicle and not the drug per se. Corn oil has been found to markedly delay the absorption of force-fed CCl_4 from the GI tract in rats (53).

The best 5-member classifier identified in our human toxicity study (AGXT, ALDOB, CRP, FBP1 and MMP9) showed better diagnostic performance than ALT and AST. Twelve of the 14 patients were correctly identified by the 5-protein panel while the ALT test detected only 3 (Figure 3). The much lower performance of ALT is probably due to its short half-life in the blood. Patients come to clinic with different dosages, post exposure times and pathologies, which are known to affect the diagnostic accuracy of ALT and AST. The new panel with liver-enriched proteins may have longer half-life, specifically linked to liver injury and less affected by other factors. The clinical utility of these markers is currently unclear but they have many possible applications. For example, one possible use of these markers may be to assess the effectiveness and prognosis of NAC treatment after APAP overdose.

Blood bathes all organs of the body, which synthesize as well as secrete/release proteins and other molecules, including small molecules and nucleic acids, into blood. In pathological conditions the profile of molecular exchange between organs and blood will be affected as a consequence of their cognate networks becoming perturbed by diseases (or toxins); therefore, analyzing the changes of molecular profiles in blood may serve as an informative window to distinguish health and disease and to provide basic insights into the pathophysiology of the disease. The approach we adopted by monitoring the change in the concentrations of organ-enriched proteins in blood is especially informative because these proteins specifically reflect disease-affected organs –hence they provide direct insights into the pathophysiology and severity of the disease. Many new potential blood markers identified in this study performed better in reflecting drug-induced liver injury than traditional blood AST and ALT measurements. Using

this approach, more informative and accurate blood markers can be identified. High quality antibodies, aptamers or synthetic capture agents against these proteins can then be developed and incorporated in devices to detect a set of diseases, including drug-induced injuries. (54). The development of microfluidic devices offer the possibility of using a fraction of a droplet of blood for such assessment—thus making it easier to follow the dynamics of the disease with frequent blood samplings. These diagnostic platforms may provide the foundation for convenient, low cost, Point-of-Care and even possibly self-administered tests which is a key step toward the contemporary predictive, preventive, personalized, and participatory (P4) medicine (55).

SUPPORTING INFORMATION:

The following files are available free of charge at ACS website http://pubs.acs.org:

Supplementary Materials-Qin et al.docx. Supplementary Methods and Figures. **Figure S1**: Characterizing individual SRM assays for the 5 informative proteins and ALT, AST in APAP overdose patients; **Figure S2**: Detection of endogenous peptide VNEAACDIAR after APAP or CCl4 treatment in mouse plasma; **Figure S3**: Collision energy optimization of 185 peptides

Supplementary Tables S1-S7 - Qin et al.xlsx. **Table S1**: Number of mice in each treatment group; **Table S2**: Information for 14 APAP overdose patients; **Table S3**: Numbers of targeted proteins and their proteotypic peptides (Protein/Peptide) filtered for SRM in each step of target protein selection; **Table S4.1**: SRM methods to monitor mouse liver proteins in APAP and CCL4 liver-toxicity mouse models; **Table S4.2**: SRM methods to monitor human liver proteins in APAP overdose serum samples; **Table S5**: No relationship between plasma APAP concentration in blood and liver injury after APAP injection; **Table S6**: Total Glutathione concentration and

GSH/GSSG ratio in 5 NOD mice at drug administration; **Table S7**: Fold change of 23 level-up proteins in individual APAP overdose patients measured by SRM as compared to healthy volunteer controls.

ACKNOWLEDGMENTS

The mouse model study was supported by DOD contract "Blood Biomarkers for Assessing the Exposure and Responses of Mammals to Chemical and Biological Agents" W911SR-06-C-0057, W911SR-07-C-0101, W911SR-09-C-0062. Human SRM research reported in this publication was performed in part with federal funds from the American Recovery and Reinvestment Act (ARRA) funds through National Institutes of Health, from the National Human Genome Research Institute grant No. RC2 HG005805, the National Institute of General Medical Sciences under grant No. R01 GM087221, 2P50 GM076547/Center for Systems Biology), the European DAAD (fellowship to UK), U54ES017885 and RM-08-029 (GSO), and DOD research contracts W911NF-10-2-0111 and HDTRA1-13-C-0055. We thank the Luxembourg Centre for Systems Biomedicine and the University of Luxembourg for supporting the Acetaminophen-overdose patient study. We also thank the MRC Centre for Drug Safety Science in Liverpool (UK) for funding the patient study. MP is a NIHR Senior Investigator. The authors thank Trevor Baker, ISB Proteomics Core, and David Rodriguez and Wiley Lawhead, for excellent technical assistance and for providing excellent husbandry care and drug injection for the mouse model study. Special thanks are given to Drs. Kelly Hudkins and Ying-Tzang Tien, University of Washington Pathology Research Service Laboratory, for providing expertise in histologic staining and analyzing the mouse liver samples.

ABBREVIATIONS

ALT, Alanine Aminotransferase; APAP, acetaminophen; AST, Aspartate Aminotransferase; C57BL/6J, B6; CCl_4, carbon tetrachloride; DILI, drug-induced liver injury; LC-IMS-MS, liquid chromatography-ion mobility spectrometry-mass spectrometry; NOD, NOD/ShiLtJ; SRM, selected reaction monitoring; WB, Western Blot.

References

1. McJunkin, B.; Barwick, K. W.; Little, W. C.; Winfield, J. B., Fatal massive hepatic necrosis following acetaminophen overdose. *JAMA* **1976,** 236, (16), 1874-5.
2. Larson, A. M.; Polson, J.; Fontana, R. J.; Davern, T. J.; Lalani, E.; Hynan, L. S.; Reisch, J. S.; Schiodt, F. V.; Ostapowicz, G.; Shakil, A. O.; Lee, W. M.; Acute Liver Failure Study, G., Acetaminophen-induced acute liver failure: results of a United States multicenter, prospective study. *Hepatology* **2005,** 42, (6), 1364-72.
3. Dart, R. C.; Erdman, A. R.; Olson, K. R.; Christianson, G.; Manoguerra, A. S.; Chyka, P. A.; Caravati, E. M.; Wax, P. M.; Keyes, D. C.; Woolf, A. D.; Scharman, E. J.; Booze, L. L.; Troutman, W. G.; American Association of Poison Control, C., Acetaminophen poisoning: an evidence-based consensus guideline for out-of-hospital management. *Clin Toxicol (Phila)* **2006,** 44, (1), 1-18.
4. Nissen, N. I.; Ranlov, P.; Weis-Fogh, J., Evaluation of Four Different Serum Enzymes in the Diagnosis of Acute Myocardial Infarction. *Br Heart J* **1965,** 27, 520-6.
5. Lindblom, P.; Rafter, I.; Copley, C.; Andersson, U.; Hedberg, J. J.; Berg, A. L.; Samuelsson, A.; Hellmold, H.; Cotgreave, I.; Glinghammar, B., Isoforms of alanine aminotransferases in human tissues and serum--differential tissue expression using novel antibodies. *Arch Biochem Biophys* **2007,** 466, (1), 66-77.
6. Dufour, D. R.; Lott, J. A.; Nolte, F. S.; Gretch, D. R.; Koff, R. S.; Seeff, L. B., Diagnosis and monitoring of hepatic injury. I. Performance characteristics of laboratory tests. *Clin Chem* **2000,** 46, (12), 2027-49.
7. Antoine, D. J.; Jenkins, R. E.; Dear, J. W.; Williams, D. P.; McGill, M. R.; Sharpe, M. R.; Craig, D. G.; Simpson, K. J.; Jaeschke, H.; Park, B. K., Molecular forms of HMGB1 and keratin-18 as mechanistic biomarkers for mode of cell death and prognosis during clinical acetaminophen hepatotoxicity. *J Hepatol* **2012,** 56, (5), 1070-9.
8. Zhou, Y. Q., S.; Wang, K., Biomarkers of drug-induced liver injury. Current Biomarker Findings. *Current Biomarker Findings* **2013,** 3, 1-9.
9. Wang, K.; Yuan, Y.; Li, H.; Cho, J. H.; Huang, D.; Gray, L.; Qin, S.; Galas, D. J., The spectrum of circulating RNA: a window into systems toxicology. *Toxicol Sci* **2013,** 132, (2), 478-92.
10. Szabo, G.; Bala, S., MicroRNAs in liver disease. *Nat Rev Gastroenterol Hepatol* **2013,** 10, (9), 542-52.
11. Huttenhain, R.; Soste, M.; Selevsek, N.; Rost, H.; Sethi, A.; Carapito, C.; Farrah, T.; Deutsch, E. W.; Kusebauch, U.; Moritz, R. L.; Nimeus-Malmstrom, E.; Rinner, O.; Aebersold, R., Reproducible quantification of cancer-associated proteins in body fluids using targeted proteomics. *Sci Transl Med* **2012,** 4, (142), 142ra94.
12. Picotti, P.; Aebersold, R., Selected reaction monitoring-based proteomics: workflows, potential, pitfalls and future directions. *Nat Methods* **2012,** 9, (6), 555-66.
13. Carr, S. A.; Abbatiello, S. E.; Ackermann, B. L.; Borchers, C.; Domon, B.; Deutsch, E. W.; Grant, R. P.; Hoofnagle, A. N.; Huttenhain, R.; Koomen, J. M.; Liebler, D. C.; Liu, T.; MacLean, B.; Mani, D. R.; Mansfield, E.; Neubert, H.; Paulovich, A. G.; Reiter, L.; Vitek, O.; Aebersold, R.; Anderson, L.; Bethem, R.; Blonder, J.; Boja, E.; Botelho, J.; Boyne, M.; Bradshaw, R. A.; Burlingame, A. L.; Chan, D.; Keshishian, H.; Kuhn, E.; Kinsinger, C.; Lee, J. S.; Lee, S. W.; Moritz, R.; Oses-Prieto, J.; Rifai, N.; Ritchie, J.; Rodriguez, H.; Srinivas, P. R.; Townsend, R. R.; Van Eyk, J.; Whiteley, G.; Wiita, A.; Weintraub, S., Targeted peptide measurements in biology and medicine: best practices for mass spectrometry-based assay development using a fit-for-purpose approach. *Mol Cell Proteomics* **2014,** 13, (3), 907-17.
14. Mirochnitchenko, O.; Weisbrot-Lefkowitz, M.; Reuhl, K.; Chen, L.; Yang, C.; Inouye, M., Acetaminophen toxicity. Opposite effects of two forms of glutathione peroxidase. *J Biol Chem* **1999,** 274, (15), 10349-55.
15. Simpson, K.; Hogaboam, C. M.; Kunkel, S. L.; Harrison, D. J.; Bone-Larson, C.; Lukacs, N. W., Stem cell factor attenuates liver damage in a murine model of acetaminophen-induced hepatic injury. *Lab Invest* **2003,** 83, (2), 199-206.
16. Yu, C.; Wang, F.; Jin, C.; Wu, X.; Chan, W. K.; McKeehan, W. L., Increased carbon tetrachloride-induced liver injury and fibrosis in FGFR4-deficient mice. *Am J Pathol* **2002,** 161, (6), 2003-10.
17. Nath, R. G.; Li, D. H.; Randerath, K., Acute and long-term effects of carbon tetrachloride on DNA modifications (I-compounds) in male mouse liver. *Chem Biol Interact* **1990,** 76, (3), 343-57.
18. Tammen, H., Specimen collection and handling: standardization of blood sample collection. *Methods Mol Biol* **2008,** 428, 35-42.
19. Doumas, B.; Biggs, H. G., A colorimetric method for assaying serum aspartate aminotransferase activities. *Clin Chim Acta* **1969,** 23, (1), 75-82.
20. Henry, R. J.; Chiamori, N.; Golub, O. J.; Berkman, S., Revised spectrophotometric methods for the determination of glutamic-oxalacetic transaminase, glutamic-pyruvic transaminase, and lactic acid dehydrogenase. *Am J Clin Pathol* **1960,** 34, 381-98.

21. Qin, S.; Zhou, Y.; Lok, A. S.; Tsodikov, A.; Yan, X.; Gray, L.; Yuan, M.; Moritz, R. L.; Galas, D.; Omenn, G. S.; Hood, L., SRM targeted proteomics in search for biomarkers of HCV-induced progression of fibrosis to cirrhosis in HALT-C patients. *Proteomics* **2012,** 12, (8), 1244-52.
22. Zhang, Q.; Menon, R.; Deutsch, E. W.; Pitteri, S. J.; Faca, V. M.; Wang, H.; Newcomb, L. F.; Depinho, R. A.; Bardeesy, N.; Dinulescu, D.; Hung, K. E.; Kucherlapati, R.; Jacks, T.; Politi, K.; Aebersold, R.; Omenn, G. S.; States, D. J.; Hanash, S. M., A mouse plasma peptide atlas as a resource for disease proteomics. *Genome Biol* **2008,** 9, (6), R93.
23. Kusebauch, U.; Campbell, D. S.; Deutsch, E. W.; Chu, C. S.; Spicer, D. A.; Brusniak, M. Y.; Slagel, J.; Sun, Z.; Stevens, J.; Grimes, B.; Shteynberg, D.; Hoopmann, M. R.; Blattmann, P.; Ratushny, A. V.; Rinner, O.; Picotti, P.; Carapito, C.; Huang, C. Y.; Kapousouz, M.; Lam, H.; Tran, T.; Demir, E.; Aitchison, J. D.; Sander, C.; Hood, L.; Aebersold, R.; Moritz, R. L., Human SRMAtlas: A Resource of Targeted Assays to Quantify the Complete Human Proteome. *Cell* **2016,** 166, (3), 766-78.
24. MacLean, B.; Tomazela, D. M.; Shulman, N.; Chambers, M.; Finney, G. L.; Frewen, B.; Kern, R.; Tabb, D. L.; Liebler, D. C.; MacCoss, M. J., Skyline: an open source document editor for creating and analyzing targeted proteomics experiments. *Bioinformatics* **2010,** 26, (7), 966-8.
25. Li, X. J.; Hayward, C.; Fong, P. Y.; Dominguez, M.; Hunsucker, S. W.; Lee, L. W.; McLean, M.; Law, S.; Butler, H.; Schirm, M.; Gingras, O.; Lamontagne, J.; Allard, R.; Chelsky, D.; Price, N. D.; Lam, S.; Massion, P. P.; Pass, H.; Rom, W. N.; Vachani, A.; Fang, K. C.; Hood, L.; Kearney, P., A blood-based proteomic classifier for the molecular characterization of pulmonary nodules. *Sci Transl Med* **2013,** 5, (207), 207ra142.
26. Saeed, A. I.; Sharov, V.; White, J.; Li, J.; Liang, W.; Bhagabati, N.; Braisted, J.; Klapa, M.; Currier, T.; Thiagarajan, M.; Sturn, A.; Snuffin, M.; Rezantsev, A.; Popov, D.; Ryltsov, A.; Kostukovich, E.; Borisovsky, I.; Liu, Z.; Vinsavich, A.; Trush, V.; Quackenbush, J., TM4: a free, open-source system for microarray data management and analysis. *Biotechniques* **2003,** 34, (2), 374-8.
27. Davidson, D. G.; Eastham, W. N., Acute liver necrosis following overdose of paracetamol. *Br Med J* **1966,** 2, (5512), 497-9.
28. Boyd, E. M.; Bereczky, G. M., Liver necrosis from paracetamol. *Br J Pharmacol Chemother* **1966,** 26, (3), 606-14.
29. Ansher, S. S.; Dolan, P.; Bueding, E., Chemoprotective effects of two dithiolthiones and of butylhydroxyanisole against carbon tetrachloride and acetaminophen toxicity. *Hepatology* **1983,** 3, (6), 932-5.
30. Gorla, N.; de Ferreyra, E. C.; Villarruel, M. C.; de Fenos, O. M.; Castro, J. A., Studies on the mechanism of glutathione prevention of carbon tetrachloride-induced liver injury. *Br J Exp Pathol* **1983,** 64, (4), 388-95.
31. Micheel, C. M.; Nass, S. J.; Omenn, G. S., Committee on the Review of Omics-Based Tests for Predicting Patient Outcomes in Clinical Trials. In *Evolution of Translational Omics: Lessons Learned and the Path Forward*. National Academies Press (US): Washington (DC), 2012; p 274 pp.
32. Harrill, A. H.; Watkins, P. B.; Su, S.; Ross, P. K.; Harbourt, D. E.; Stylianou, I. M.; Boorman, G. A.; Russo, M. W.; Sackler, R. S.; Harris, S. C.; Smith, P. C.; Tennant, R.; Bogue, M.; Paigen, K.; Harris, C.; Contractor, T.; Wiltshire, T.; Rusyn, I.; Threadgill, D. W., Mouse population-guided resequencing reveals that variants in CD44 contribute to acetaminophen-induced liver injury in humans. *Genome Res* **2009,** 19, (9), 1507-15.
33. Lim, A. Y.; Segarra, I.; Chakravarthi, S.; Akram, S.; Judson, J. P., Histopathology and biochemistry analysis of the interaction between sunitinib and paracetamol in mice. *BMC Pharmacol* **2010,** 10, 14.
34. Liu, W. X.; Jia, F. L.; He, Y. Y.; Zhang, B. X., Protective effects of 5-methoxypsoralen against acetaminophen-induced hepatotoxicity in mice. *World J Gastroenterol* **2012,** 18, (18), 2197-202.
35. Irie, H.; Asano-Hoshino, A.; Sekino, Y.; Nogami, M.; Kitagawa, T.; Kanda, H., Striking LD50 variation associated with fluctuations of CYP2E1-positive cells in hepatic lobule during chronic CCl4 exposure in mice. *Virchows Arch* **2010,** 456, (4), 423-31.
36. Burk, R. F., Glutathione-dependent protection by rat liver microsomal protein against lipid peroxidation. *Biochim Biophys Acta* **1983,** 757, (1), 21-8.
37. Clayton, T. A.; Baker, D.; Lindon, J. C.; Everett, J. R.; Nicholson, J. K., Pharmacometabonomic identification of a significant host-microbiome metabolic interaction affecting human drug metabolism. *Proc Natl Acad Sci U S A* **2009,** 106, (34), 14728-33.
38. Sun, B.; Utleg, A. G.; Hu, Z.; Qin, S.; Keller, A.; Lorang, C.; Gray, L.; Brightman, A.; Lee, D.; Alexander, V. M.; Ranish, J. A.; Moritz, R. L.; Hood, L., Glycocapture-assisted global quantitative proteomics (gagQP) reveals multiorgan responses in serum toxicoproteome. *J Proteome Res* **2013,** 12, (5), 2034-44.
39. Knittel, T.; Mehde, M.; Grundmann, A.; Saile, B.; Scharf, J. G.; Ramadori, G., Expression of matrix metalloproteinases and their inhibitors during hepatic tissue repair in the rat. *Histochem Cell Biol* **2000,** 113, (6), 443-53.

40. Asaka, M.; Miyazaki, T.; Hollinger, F. B.; Alpert, E., Human aldolase B serum levels: a marker of liver injury. *Hepatology* **1984,** 4, (3), 531-5.
41. Racine-Samson, L.; Scoazec, J. Y.; D'Errico, A.; Fiorentino, M.; Christa, L.; Moreau, A.; Roda, C.; Grigioni, W. F.; Feldman, G., The metabolic organization of the adult human liver: a comparative study of normal, fibrotic, and cirrhotic liver tissue. *Hepatology* **1996,** 24, (1), 104-13.
42. McGill, M. R.; Sharpe, M. R.; Williams, C. D.; Taha, M.; Curry, S. C.; Jaeschke, H., The mechanism underlying acetaminophen-induced hepatotoxicity in humans and mice involves mitochondrial damage and nuclear DNA fragmentation. *J Clin Invest* **2012,** 122, (4), 1574-83.
43. Clyne, B.; Olshaker, J. S., The C-reactive protein. *J Emerg Med* **1999,** 17, (6), 1019-25.
44. McGill, M. R.; Cao, M.; Svetlov, A.; Sharpe, M. R.; Williams, C. D.; Curry, S. C.; Farhood, A.; Jaeschke, H.; Svetlov, S. I., Argininosuccinate synthetase as a plasma biomarker of liver injury after acetaminophen overdose in rodents and humans. *Biomarkers* **2014,** 19, (3), 222-30.
45. Kuo, F. C.; Hwu, W. L.; Valle, D.; Darnell, J. E., Jr., Colocalization in pericentral hepatocytes in adult mice and similarity in developmental expression pattern of ornithine aminotransferase and glutamine synthetase mRNA. *Proc Natl Acad Sci U S A* **1991,** 88, (21), 9468-72.
46. Mato, J. M.; Martinez-Chantar, M. L.; Lu, S. C., Methionine metabolism and liver disease. *Annu Rev Nutr* **2008,** 28, 273-93.
47. Janke, R.; Dodson, A. E.; Rine, J., Metabolism and epigenetics. *Annu Rev Cell Dev Biol* **2015,** 31, 473-96.
48. Zanger, U. M.; Schwab, M., Cytochrome P450 enzymes in drug metabolism: regulation of gene expression, enzyme activities, and impact of genetic variation. *Pharmacol Ther* **2013,** 138, (1), 103-41.
49. Chen, L.; Zeng, Y.; Yang, H.; Lee, T. D.; French, S. W.; Corrales, F. J.; Garcia-Trevijano, E. R.; Avila, M. A.; Mato, J. M.; Lu, S. C., Impaired liver regeneration in mice lacking methionine adenosyltransferase 1A. *FASEB J* **2004,** 18, (7), 914-6.
50. Lisman, T.; Porte, R. J., Rebalanced hemostasis in patients with liver disease: evidence and clinical consequences. *Blood* **2010,** 116, (6), 878-85.
51. Knockaert, L.; Berson, A.; Ribault, C.; Prost, P. E.; Fautrel, A.; Pajaud, J.; Lepage, S.; Lucas-Clerc, C.; Begue, J. M.; Fromenty, B.; Robin, M. A., Carbon tetrachloride-mediated lipid peroxidation induces early mitochondrial alterations in mouse liver. *Lab Invest* **2012,** 92, (3), 396-410.
52. Aleksunes, L. M.; Slitt, A. M.; Cherrington, N. J.; Thibodeau, M. S.; Klaassen, C. D.; Manautou, J. E., Differential expression of mouse hepatic transporter genes in response to acetaminophen and carbon tetrachloride. *Toxicol Sci* **2005,** 83, (1), 44-52.
53. Kim, H. J.; Bruckner, J. V.; Dallas, C. E.; Gallo, J. M., Effect of dosing vehicles on the pharmacokinetics of orally administered carbon tetrachloride in rats. *Toxicol Appl Pharmacol* **1990,** 102, (1), 50-60.
54. Fan, R.; Vermesh, O.; Srivastava, A.; Yen, B. K.; Qin, L.; Ahmad, H.; Kwong, G. A.; Liu, C. C.; Gould, J.; Hood, L.; Heath, J. R., Integrated barcode chips for rapid, multiplexed analysis of proteins in microliter quantities of blood. *Nat Biotechnol* **2008,** 26, (12), 1373-8.
55. Hood, L., Systems biology and p4 medicine: past, present, and future. *Rambam Maimonides Med J* **2013,** 4, (2), e0012.

Tables

Table 1. Summary of SRM analyses of the 49 informative proteins in plasma and liver tissue of NOD mice treated with APAP or CCl_4. Existing liver injury markers ALT (ALT1), AST1 and AST2 showed significant elevations in treated plasma samples compared to controls. T-test was used to determine the significance of concentration change of specific proteins between treated and control at pre-peak response time (3h for APAP or 3-8h for CCl_4), at peak response time (8-24h for APAP or 24-48h for CCl_4) and at post-peak response time (48-96h for APAP or 72-96h for CCl_4). Significant inter-individual variation negatively affected *p*-values in APAP-treated mice. Exact fold changes at data points (average of two peptides) in concentration increase category of the most hyper-response mouse plasma were specified.

ND: not detected, ↑ concentration increase, ↓ concentration decrease, Blank: no change.

		Plasma					Liver			
Gene name	**Drug**	**Pre-peak response time**	**Peak response time**	**Post-peak response time**	**Treat vs. control**	**Fold increase compared to average of controls**	**Pre-peak response time**	**Peak response time**	**Post-peak response time**	**Treat vs. control**
Protein Up										
Agxt	APAP		↑ p<0.05		↑ p<0.05	3h2 6X, 48h2 43X, 72h4 35X, 96h2 5X	↓ p<0.01	↓ p<0.01	↓ p<0.01	↓ p<0.01
	CCl_4		↑ p<0.01		↑ p<0.01					
Aldh1a1	APAP	↑ p<0.05	↑ p<0.01	↑ p<0.05	↑ p<0.01	3h2 5X, 48h2 24X, 72h4 50X, 96h2 25X	↓ p<0.01	↓ p<0.01		↓ p<0.05
	CCl_4		↑ p<0.01	↑ p<0.05	↑ p<0.01			↓ p<0.05		
Aldob	APAP		↑ p<0.01		↑ p<0.01	48h2 84X, 72h4 201X				
	CCl_4		↑ p<0.01		↑ p<0.05				↓ p<0.01	
ALT	APAP		↑ p<0.05		↑ p<0.01	48h2 16X, 72h4 32X	↓ p<0.01	↓ p<0.01	↓ p<0.01	↓ p<0.01
	CCl_4		↑ p<0.05	↑ p<0.05	↑ p<0.05			↓ p<0.05		
Apob	APAP			↑ p<0.05		48h2 4X, 72h4 2X			↓ p<0.05	
	CCl_4			↑ p<0.05					↓ p<0.05	
Asl	APAP		↑ p<0.05		↑ p<0.05	48h2 71X, 72h4 122X, 96h4 9X				
	CCl_4		↑ p<0.01		↑ p<0.05				↓ p<0.01	
Ass1	APAP		↑ p<0.05		↑ p<0.01	3h2 7X, 48h2 152X, 72h4 204X, 96h4 13X			↓ p<0.05	
	CCl_4		↑ p<0.01	↑ p<0.05	↑ p<0.01				↓ p<0.05	
Ast1	APAP		↑ p<0.05		↑ p<0.05	48h2 4X, 72h4 7X				
	CCl_4		↑ p<0.01		↑ p<0.05				↓ p<0.05	
Ast2	APAP		↑ p<0.01		↑ p<0.05	48h2 13X, 72h4 86X	↓ p<0.01	↓ p<0.01	↓ p<0.01	↓ p<0.01
	CCl_4		↑ p<0.01	↑ p<0.05	↑ p<0.05					
Bhmt	APAP		↑ p<0.05		↑ p<0.05	3h2 17X, H8048h2 50X, 72h4 204X, 96h4 8X	↓ p<0.01	↓ p<0.01	↓ p<0.01	↓ p<0.01
	CCl_4		↑ p<0.01	↑ p<0.01	↑ p<0.05			↓ p<0.01	↓ p<0.05	
Cat	APAP		↑ p<0.05		↑ p<0.01	48h2 29X, 72h4 28X				
	CCl_4	↑ p<0.05	↑ p<0.01	↑ p<0.01	↑ p<0.05					
Dpys	APAP		↑ p<0.01		↑ p<0.01	48h2 119X, 72h4 249X, 96h4 6X				
	CCl_4		↑ p<0.01	↑ p<0.05	↑ p<0.01					
Fah	APAP	↑ p<0.01	↑ p<0.05		↑ p<0.01	3h2 4X, 48h2 55X, 72h4 115X, 96h4 6X	↓ p<0.01	↓ p<0.01	↓ p<0.05	↓ p<0.05
	CCl_4		↑ p<0.05	↑ p<0.01	↑ p<0.01					
Fbp1	APAP		↑ p<0.05		↑ p<0.05	3h2 3X, 48h2 6X, 72h4 150X		↓ p<0.01	↓ p<0.01	↓ p<0.01
	CCl_4		↑ p<0.01		↑ p<0.05					
Glud1	APAP			↑ p<0.05	↑ p<0.05	48h2 761X, 72h4 1465X, 96h4 138X				
	CCl_4		↑ p<0.01	↑ p<0.01	↑ p<0.01					
Gnmt	APAP		↑ p<0.05		↑ p<0.05	3h2 5X, 48h2 65X, 72h4 220X, 96h4 4X	↓ p<0.05	↓ p<0.05	↓ p<0.05	↓ p<0.05
	CCl_4		↑ p<0.01		↑ p<0.05					
Hgd	APAP	↑ p<0.01	↑ p<0.01		↑ p<0.05	48h2 63X, 72h4 145X	↓ p<0.01	↓ p<0.01	↓ p<0.01	↓ p<0.01
	CCl_4		↑ p<0.01		↑ p<0.05			↓ p<0.01		↓ p<0.05
Hmgcs2	APAP		↑ p<0.05		↑ p<0.05	48h2 12X, 72h4 24X, 96h4 3X				
	CCl_4		↑ p<0.01	↑ p<0.05	↑ p<0.01				↓ p<0.01	
Hpd	APAP	↑ p<0.01	↑ p<0.05		↑ p<0.05	48h2 6X, 72h4 23X	↓ p<0.01	↓ p<0.01	↓ p<0.01	↓ p<0.01
	CCl_4		↑ p<0.01		↑ p<0.05			↓ p<0.01	↓ p<0.01	↓ p<0.01
Idh1	APAP		↑ p<0.05		↑ p<0.05	48h2 4X, 72h4 23X				
	CCl_4		↑ p<0.01		↑ p<0.05					
Mat1a	APAP		↑ p<0.05		↑ p<0.05	3h2 8X, 48h2 22X, 72h4 32X, 96h4 3X	↓ p<0.05	↓ p<0.05		
	CCl_4		↑ p<0.01	↑ p<0.05	↑ p<0.01				↓ p<0.01	↓ p<0.05
Mdh1	APAP		↑ p<0.05		↑ p<0.05	48h2 2X, 72h4 9X+H44	↓ p<0.01	↓ p<0.01	↓ p<0.01	↓ p<0.01
	CCl_4		↑ p<0.01		↑ p<0.05			↓ p<0.05		
Sardh	APAP		↑ p<0.05		↑ p<0.05	48h2 6X, 72h4 13X				
	CCl_4		↑ p<0.05		↑ p<0.05				↓ p<0.05	
Ubp1	APAP		↑ p<0.05	↑ p<0.05	↑ p<0.05					
	CCl_4	↑ p<0.05	↑ p<0.01		↑ p<0.05					
Uroc1	APAP	↑ p<0.01	↑ p<0.05		↑ p<0.05	48h2 3X, 72h4 11X		↓ p<0.01	↓ p<0.05	↓ p<0.01
	CCl_4		↑ p<0.01		↑ p<0.05					

		Plasma					Liver			
Gene name	**Drug**	**Pre-peak response time**	**Peak response time**	**Post-peak response time**	**Treat vs. control**	**Fold increase compared to average of controls**	**Pre-peak response time**	**Peak response time**	**Post-peak response time**	**Treat vs. control**
Proteins Down										
Apcs	APAP		↓ p<0.01	↓ p<0.01			ND	ND	ND	ND
	CCl_4		↓ p<0.05				ND	ND	ND	ND
Apoa1	APAP	↓ p<0.01			↓ p<0.05				↓ p<0.05	↓ p<0.05
	CCl_4		↓ p<0.01							
C8g	APAP	↓ p<0.01	↓ p<0.01	↓ p<0.01	↓ p<0.01		ND	ND	ND	ND
	CCl_4	↓ p<0.05	↓ p<0.01		↓ p<0.05		ND	ND	ND	ND
Cfb	APAP	↓ p<0.05	↓ p<0.01		↓ p<0.05		ND	ND	ND	ND
	CCl_4		↓ p<0.01		↓ p<0.05		ND	ND	ND	ND
Cp	APAP	↓ p<0.05	↓ p<0.01	↑ p<0.01			ND	ND	ND	ND
	CCl_4			↑ p<0.05			ND	ND	ND	ND
Cpb2	APAP	↓ p<0.01	↓ p<0.01		↓ p<0.05		↓ p<0.05	↓ p<0.01		
	CCl_4	↓ p<0.01	↓ p<0.01		↓ p<0.01		↓ p<0.05			↓ p<0.05
F10	APAP	↓ p<0.01	↓ p<0.01		↓ p<0.05		ND	ND	ND	ND
	CCl_4		↓ p<0.05	↓ p<0.05	↓ p<0.05		ND	ND	ND	ND
F12	APAP	↓ p<0.01	↓ p<0.01		↓ p<0.05		ND	ND	ND	ND
	CCl_4		↓ p<0.05				ND	ND	ND	ND
F2	APAP	↓ p<0.01	↓ p<0.01		↓ p<0.05		ND	ND	ND	ND
	CCl_4		↓ p<0.01	↓ p<0.05	↓ p<0.05		ND	ND	ND	ND
Fetub	APAP		↓ p<0.05					↓ p<0.05		
	CCl_4			↓ p<0.05						
Hgfac	APAP	↓ p<0.01	↓ p<0.01		↓ p<0.05		↓ p<0.01			↓ p<0.05
	CCl_4		↓ p<0.05				↓ p<0.01		↑ p<0.05	
Hpx	APAP	↓ p<0.01	↓ p<0.01				↓ p<0.01	↓ p<0.01	↓ p<0.01	↓ p<0.01
	CCl_4	↓ p<0.01	↓ p<0.01				↓ p<0.01			
Hrg	APAP	↓ p<0.05	↓ p<0.05							
	CCl_4		↓ p<0.01					↓ p<0.01	↓ p<0.01	↓ p<0.01
Igfals	APAP	↓ p<0.01	↓ p<0.01				ND	ND	ND	ND
	CCl_4		↓ p<0.01	↓ p<0.01	↓ p<0.01		ND	ND	ND	ND
Itih1	APAP	↓ p<0.01	↓ p<0.05		↓ p<0.05					
	CCl_4		↓ p<0.01						↓ p<0.05	
Itih4	APAP	↓ p<0.05	↓ p<0.01					↓ p<0.05		
	CCl_4	↓ p<0.01	↓ p<0.01	↓ p<0.01	↓ p<0.01		↓ p<0.05			
Pglyrp2	APAP	↓ p<0.01	↓ p<0.01				ND	ND	ND	ND
	CCl_4		↓ p<0.05				ND	ND	ND	ND
plg	APAP	↓ p<0.01	↓ p<0.01		↓ p<0.01			↓ p<0.05		
	CCl_4		↓ p<0.01	↓ p<0.01	↓ p<0.01					
Rbp4	APAP	↓ p<0.01	↓ p<0.01				↓ p<0.01	↓ p<0.01	↓ p<0.01	↓ p<0.01
	CCl_4	↓ p<0.05			↓ p<0.05					
Saa4	APAP	↓ p<0.01	↓ p<0.01				ND	ND	ND	ND
	CCl_4	↓ p<0.05	↓ p<0.05		↓ p<0.05		ND	ND	ND	ND
Serpinf2	APAP	↓ p<0.01	↓ p<0.01		↓ p<0.01					
	CCl_4	↓ p<0.05	↓ p<0.01	↓ p<0.01	↓ p<0.01					
Vtn	APAP	↓ p<0.01	↓ p<0.01		↓ p<0.01					↑ p<0.05
	CCl_4	↓ p<0.05	↓ p<0.01	↓ p<0.01	↓ p<0.01			↑ p<0.05		
Proteins Down/Up										
Itih2	APAP	↓ p<0.05		↑ p<0.01				↓ p<0.01		↓ p<0.05
	CCl_4			↑ p<0.05			↓ p<0.01			
Itih3	APAP	↓ p<0.01	↓ p<0.01	↑ p<0.01			ND	ND	ND	ND
	CCl_4			↑ p<0.01	↑ p<0.05		ND	ND	ND	ND

Table 2. Fold changes of plasma ALT/AST enzyme activities and of SRM-measured proteins ALT, AST1, AST2, GLUD1, ALDOB, ASS1, BHMT. WB images for each protein in plasma were shown for APAP-treated (2A) or CCl4-treated (2B) NOD mice. The results were normalized based on the average concentrations of controls. ALT1, AST1 and AST2 protein WB bands were mainly shown at the peak responsive time points. Typical results from one animal are shown at each time point in the table. For t-test in the APAP/NOD group, all animals: 12 PBS-injected animals, mouse #1 and #2 at each of the 6 time-points from 3 hours to 96 hours post injection, and 15 APAP-treated mice (mice 03h1, 03h2, 08h1, 08h2, 08h3, 08h7, 24h1, 24h4, 24h6, 48h1, 48h2, 72h1, 72h4, 96h2, 96h4) were included. In the CCL4/NOD group, mouse #1 and #2 at each corn oil or CCl4-treated animals (12 controls and 12 treated from 3 hour to 96 hour time-points) were included. NT: not tested.

Table 2A. APAP/NOD

Time points		No treat	3h2	8h2	24h4	48h2	72h4	96h2	120h6	144h2	168h2	p value
Protein name	Method	Protein level fold change measured by SRM or enzyme activity with corresponding WB images										
ALT	Enzyme	1	2	267	98	27	55	2	1	1	1	0.01
	SRM	1	2	85	32	15	30	1	NT	NT	NT	0.02
	WB											
AST	Enzyme	1	1	73	25	4	19	1	1	2	1	0.01
AST1	SRM	1	1	39	10	3	7	1	NT	NT	NT	0.05
	WB											
AST2	SRM	1	1	2	14	13	10	1	1	1	1	0.10
	WB											
GLUD1	SRM	1	2	15	338	920	1771	168	NT	NT	NT	0.05
	WB	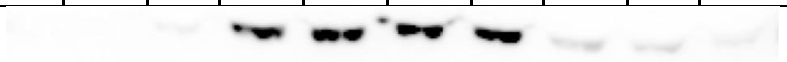										
ALDOB	SRM	1	2	124	78	13	122	1	NT	NT	NT	0.02
	WB	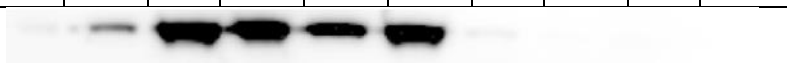										
ASS1	SRM	1	2	399	44	222	278	14	NT	NT	NT	0.03
	WB											
BHMT	SRM	1	17	942	210	69	281	9	NT	NT	NT	0.03
	WB	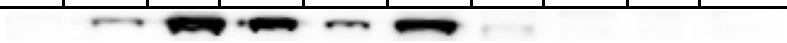										

2B. CCl4/NOD

Time points		No treat	3h1	8h1	24h1	48h1	72h1	96h1	120h1	144h1	168h1	p value
Proteins names	Method	Protein level fold change measured by SRM or enzyme activity with corresponding WB images										
ALT	Enzyme	1	2	9	583	59	4	2	1	1	1	0.03
ALT1	SRM	1	2	6	60	124	3	2	NT	NT	NT	0.06
	WB											
AST	Enzyme	1	1	6	162	6	2	2	1	1	1	0.03
AST1	SRM	1	1	3	156	196	2	1	NT	NT	NT	0.04
	WB	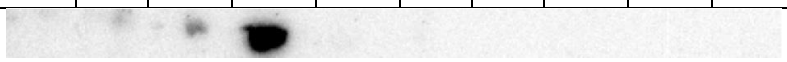										
AST2	SRM	1	1	1	163	226	6	3	NT	NT	NT	0.03
	WB	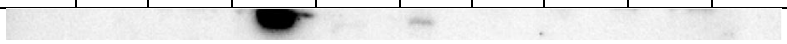										
GLUD1	SRM	1	2	2	296	366	290	235	NT	NT	NT	0.002
	WB	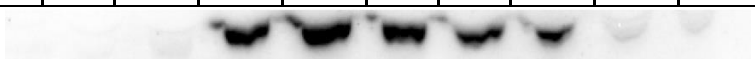										
ALDOB	SRM	1	2	11	730	635	16	2	NT	NT	NT	0.03
	WB	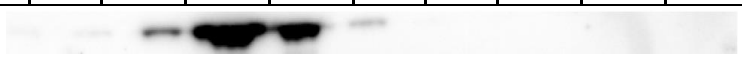										
ASS1	SRM	1	1	3	106	116	15	7	NT	NT	NT	0.01
	WB	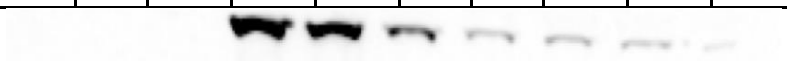										
BHMT	SRM	1	44	1451	1908	1834	72	44	NT	NT	NT	0.01
	WB	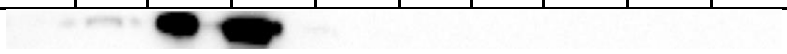										

Table 3. Agreement of concentration-increase proteins in both mouse models and human APAP overdose patients. There are 15 proteins in the human APAP overdose study that overlap with proteins in the APAP treated mouse study. 14 of the 15 proteins agree with each other with elevated protein levels (↑) after APAP exposure. APOA1 is the only exception, with decreased protein level (↓) in mouse study. NT: not tested.

Gene symbol	Human UniProtKB ID	Mouse UniProtKB ID	Protein level in human study	Protein level in mouse study
ALT	P24298	Q8QZR5	↑	↑
ADH1	P07327	P00329	↑	↑
ADH4	P08319	Q3V0P5	↑	NT
AGXT	P21549	Q8R128	↑	↑
ALDOB	P05062	Q91Y97	↑	↑
APOA1	P02647	Q8BPD5	↑	↓
APOE	P02649	P08226	↑	NT
ASS1	P00966	P16460	↑	↑
AST1	P17174	P05201	↑	↑
AST2	P00505	P05202	↑	↑
BHMT1	Q93088	O35490	↑	↑
BHMT2	Q9H2M3	Q91WS4	↑	NT
CES1	P23141	Q8VCC2	↑	NT
CRP	P02741	P14847	↑	NT
FAH	P16930	Q3TY87	↑	↑
FBP1	P09467	Q9QXD6	↑	↑
GLUD1	P00367	P26443	↑	↑
GLUD2	P49448	P26443	↑	NT
GNMT	Q14749	Q9QXF8	↑	↑
HPD	P32754	P49429	↑	↑
MAT1A	Q00266	Q91X83	↑	↑
MMP9	P14780	P41245	↑	NT
UROC1	Q96N76	Q3UEL5	↑	↑

Figure Legends

Figure 1. Significant responsiveness variation among APAP-treated B6 and NOD mice were indicated by differences of plasma ALT and AST activities. Variations after CCl4 treatment were small in both strains. **Figure 1A** shows log2 values of ALT and AST enzyme activities (IU/ml) in the APAP/B6, APAP/NOD, CCl4/B6 and CCl4/NOD groups. In the APAP groups, 10 or fewer mice were used at each time point. In the CCl4 groups, every time point has 3 (B6) or 4 (NOD) mice. Each marker in the chart of Figure 1A represents the log2 ALT or AST enzyme activity value of an individual mouse at each time point. Marked lines in Figure 1A: average ALT (black) and AST (red) levels with STDEV error bars. **Figure 1B**: Histopathology images show that liver damage 8 hours post APAP treatment correspond to the huge ALT, AST enzyme activity variations. **Figure 1B1**: Liver stain of PBS treated mouse from the APAP/NOD group shows normal liver cells. **1B2**: Liver damage characterized by severe central lobular necrosis and bleeding was observed in Mouse APAP/NOD/8h2 (NOD mouse #2 treated with APAP at 8h time point, a super responder by ALT and AST activities). **1B3**: close to normal liver structure was observed in liver slice from mouse APAP/NOD/8h1 (one of the least responders). **Figure 1C**: Histopathology images show that liver damages caused by CCl4 24 hours post treatment correspond to the ALT, AST enzyme activities without significant variation among mice in each time point group. **1C1**: Corn-oil treated mouse shows normal liver structure. **1C2** and **1C3** show livers from both mouse CCl4/NOD/24h1 and CCl4/NOD/24h2 at 24 hour time point with similar ALT, AST values are similarly damaged with severe wide spread centrilobular necrosis and hemorrhage.

Figure 2. 2A. Fold changes (Log2 value) of 25 concentration increase proteins by SRM in APAP-treated NOD mice showing consistency of SRM measurement with ALT and AST enzyme activity levels. Data normalized on negative controls (average of 12 PBS treated mice, 2 mice at each of the 6 time points). SRM results shown are average of two peptides from each protein (in some cases, only one peptide/protein). ALT and AST enzyme activity fold changes are shown as black (ALT) or red (AST) lines. **2B.** Similar to 2A, showing normalized fold-changes from concentration increase proteins after CCl_4 treatment in NOD mice. Mouse number 03h1 is mouse #1 sacrificed at 3 hour time point, 08h1 is mouse #1 sacrificed at 8 hour time point, and so on. Since mice were sacrificed at time of sample collection, mouse 03h1 is not the same mouse as 08h1 and so on. Each batch of vertical lines reflects different proteins concentrations obtained from an individual mouse at a given time point.

Figure 3. **A**. Heat map showing classifiers AGXT, ALODB, CRP, FBP1 and MMP9 detected 12 of the 14 APAP overdose patients while ALT and AST detected 3 patients. **B**. This 5 protein panel increased detection sensitivity from 0.54 to 0.85 and specificity from 0.50 to 0.84 when compared to ALT and AST. **C**. SRM results of two proteins, ALDOB and CRP, have been validated by Western blotting. SRM test results of ALDOB and CRP proteins showing fold change over healthy volunteer controls. Numbers shown in the Liver function test (LFT) with ALT are enzyme activities (IU/L) in serum not fold changes, <35 IU/L is considered as normal range of ALT. Due to number of gel well limitation, only 5 controls (HV) were randomly selected for WB except HV07 which showed a >4 fold increase of CRP in serum than control average. A combination of ALDOB and CRP detected APAP caused liver injury in 10 patients by Western blotting (high-lighted with yellow fill).

Figure 4. Informative proteins observed in plasma from the mouse DILI and human APAP patient studies were rearranged by network according to enriched annotations. Extracellular proteins were measured with decreased concentrations in mice plasma after APAP or CCl4 exposure while liver proteins with elevated concentrations in plasma were all intracellular (except A1BG, CRP and MMP9). Network analysis shows that most of these cytosolic or mitochondrial proteins are related to functions mainly localized in hepatic zone 3 where hepatocytes have the poorest oxygenation and perform oxygen-independent metabolic processes. ADH1A1, ADH4, ALDH1A1, CAT and HMGCS2, are annotated with process of response to oxidative stress and xenobiotic metabolism. Some other concentration-increase proteins discovered in this study and 2 other proteins from Ref 52 (NQO1 and HMOX1) are annotated with process of response to oxidative stress and xenobiotic metabolism that happen in zone 3.

Figures

Figure 1

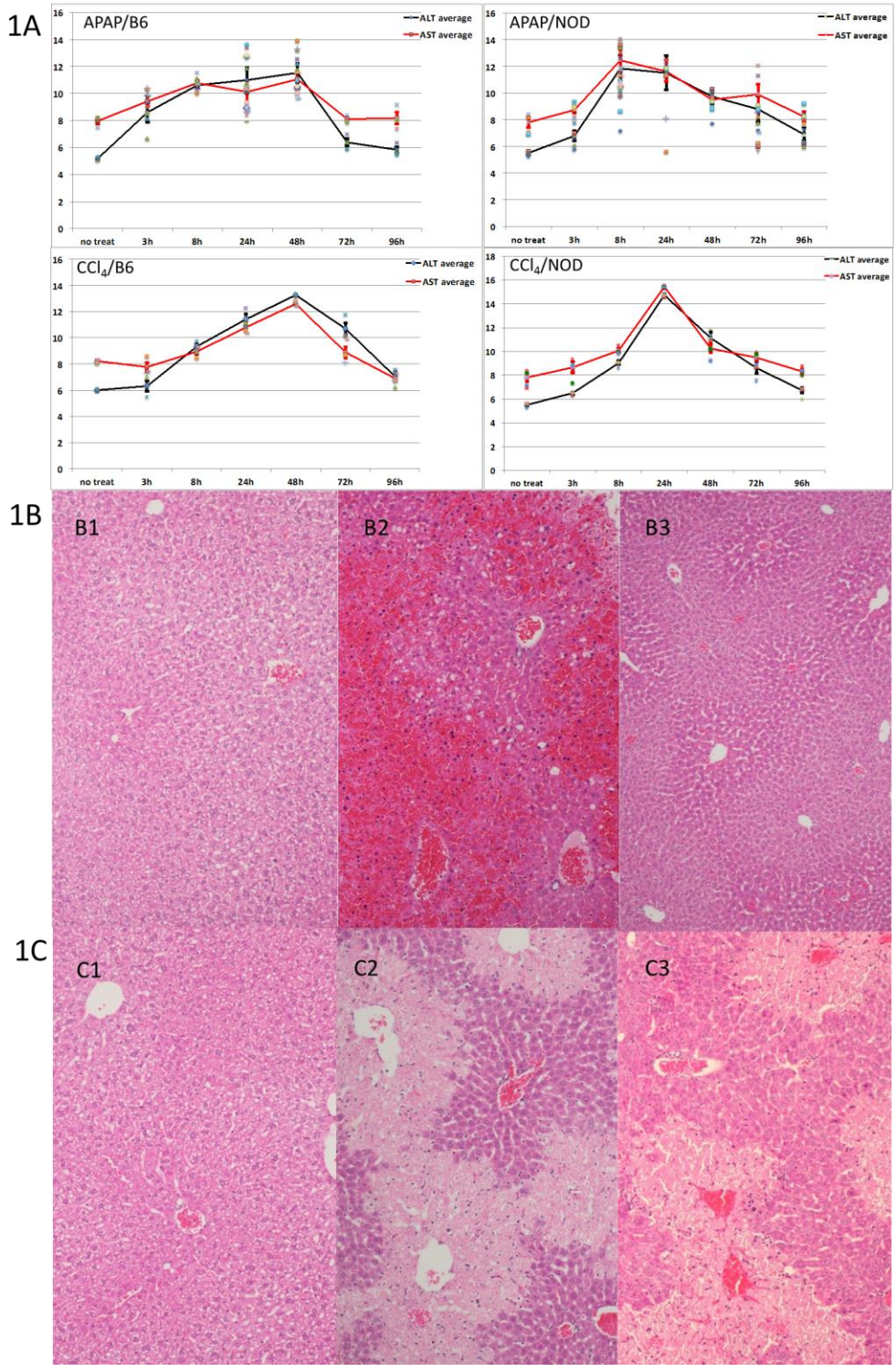

.

Figure 2

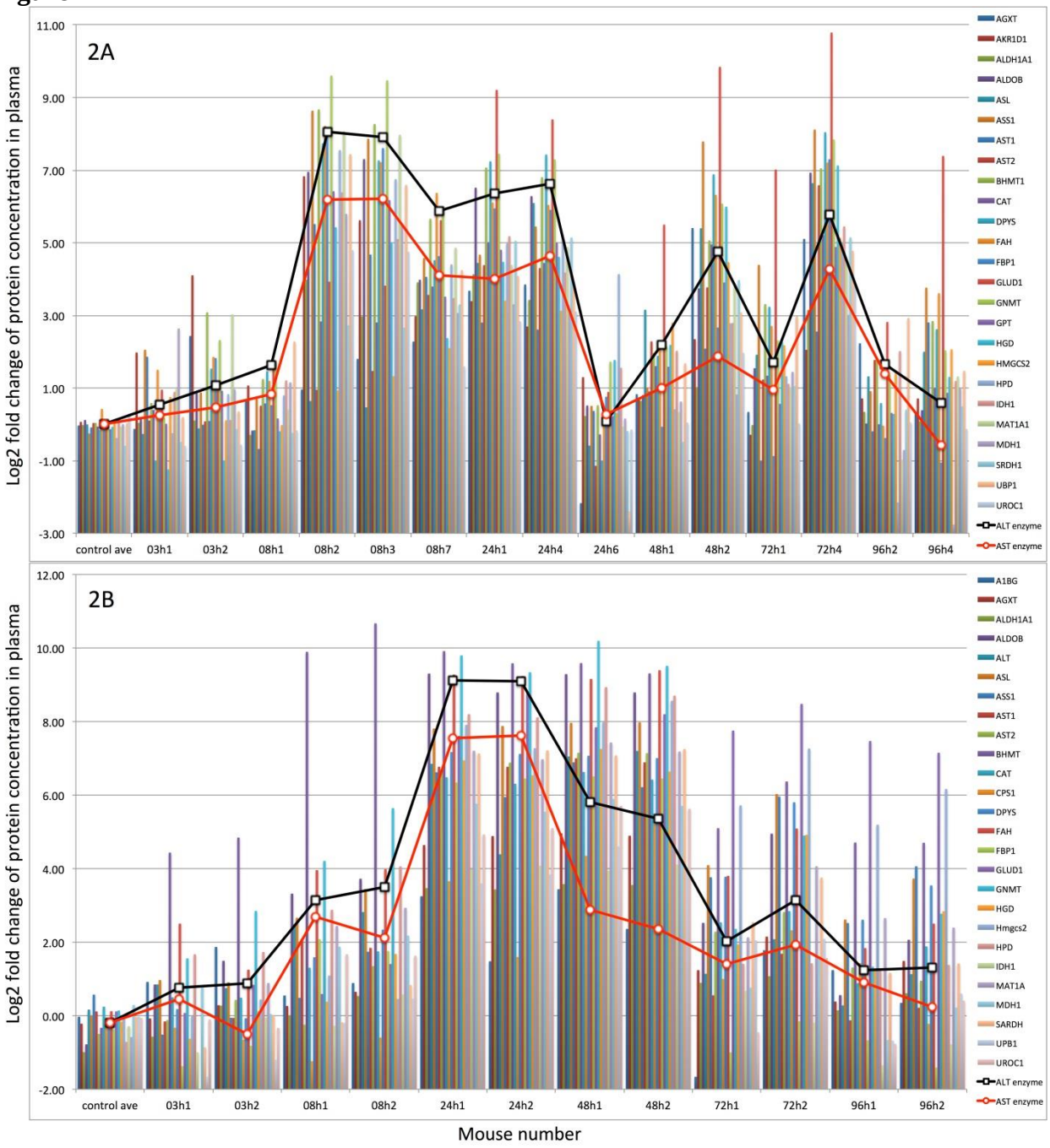
2A
Log2 fold change of protein concentration in plasma
11.00
9.00
7.00
5.00
3.00
1.00
-1.00
-3.00
control ave
03h1
03h2
08h1
08h2
08h3
08h7
24h1
24h4
24h6
48h1
48h2
72h1
72h4
96h2
96h4
AGXT
AKR1D1
ALDH1A1
ALDOB
ASL
ASS1
AST1
AST2
BHMT1
CAT
DPYS
FAH
FBP1
GLUD1
GNMT
GPT
HGD
HMGCS2
HPD
IDH1
MAT1A1
MDH1
SRDH1
UBP1
UROC1
ALT enzyme
AST enzyme
2B
Log2 fold change of protein concentration in plasma
12.00
10.00
8.00
6.00
4.00
2.00
0.00
-2.00
control ave
03h1
03h2
08h1
08h2
24h1
24h2
48h1
48h2
72h1
72h2
96h1
96h2
A1BG
AGXT
ALDH1A1
ALDOB
ALT
ASL
ASS1
AST1
AST2
BHMT
CAT
CPS1
DPYS
FAH
FBP1
GLUD1
GNMT
HGD
Hmgcs2
HPD
IDH1
MAT1A
MDH1
SARDH
UPB1
UROC1
ALT enzyme
AST enzyme
Mouse number

Figure 3.

A

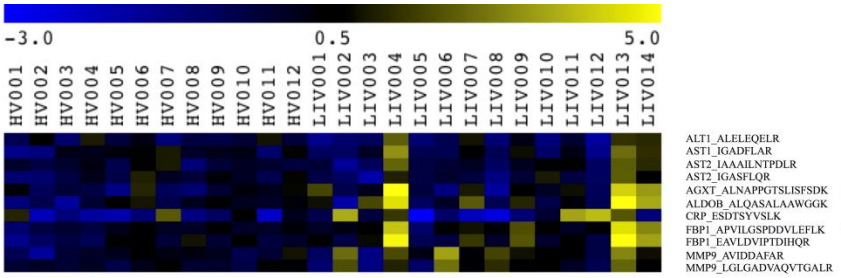

B

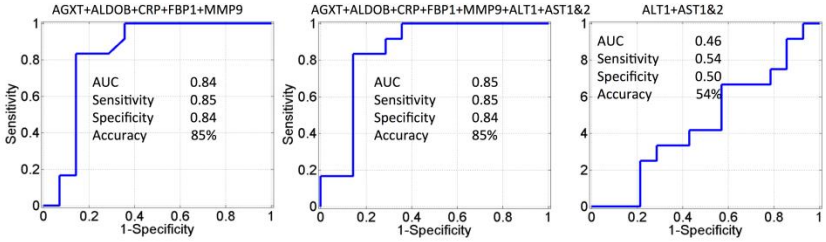

C

	HV001	HV004	HV007	HV009	HV011	LIV001	LIV002	LIV003	LIV004	LIV005	LIV006	LIV007	LIV008	LIV009	LIV010	LIV011	LIV012	LIV013	LIV014
ALT enzyme activity (IU/L)	NT	NT	NT	NT	NT	14	26	75	445	13	9	71	16	39	9	33	16	57	79
ALDOB_SRM fold change	0.4	0.9	0.7	1.3	1.0	1.8	0.3	3.5	22.7	0.6	1.0	4.3	0.7	2.3	0.7	1.2	0.6	46.8	11.6
ALDOB_WB																			
CRP_SRM fold change	2.3	0.3	4.4	0.6	0.2	0.7	11.9	0.8	2.8	0.1	0.5	0.2	0.2	0.5	0.9	10.5	14.2	4.1	0.5
CRP_WB																			

Figure 4.

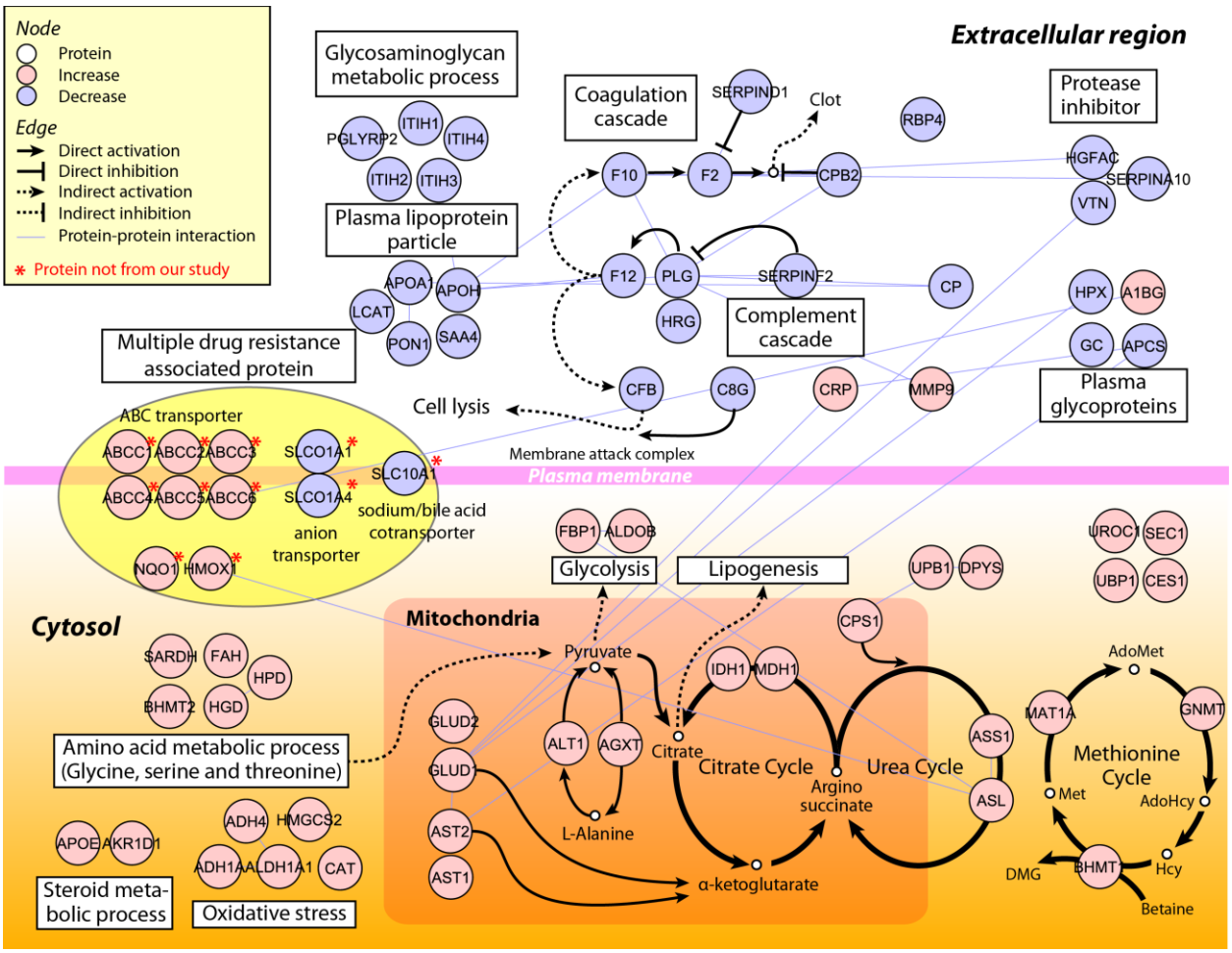
Node
Protein
Increase
Decrease
Edge
Direct activation
Direct inhibition
Indirect activation
Indirect inhibition
Protein-protein interaction
* Protein not from our study
Extracellular region
Glycosaminoglycan metabolic process
PGLYRP2
ITIH1
ITIH4
ITIH2
ITIH3
Plasma lipoprotein particle
APOA1
APOH
LCAT
PON1
SAA4
Coagulation cascade
SERPIND1
Clot
F10
F2
CPB2
RBP4
Protease inhibitor
HGFAC
SERPINA10
VTN
F12
PLG
SERPINF2
CP
HRG
Complement cascade
HPX
A1BG
GC
APCS
Plasma glycoproteins
Multiple drug resistance associated protein
ABC transporter
ABCC1
ABCC2
ABCC3
ABCC4
ABCC5
ABCC6
SLCO1A1
SLCO1A4
SLC10A1
anion transporter
sodium/bile acid cotransporter
Cell lysis
CFB
C8G
CRP
MMP9
Membrane attack complex
Plasma membrane
NQO1
HMOX1
FBP1
ALDOB
Glycolysis
Lipogenesis
UPB1
DPYS
UROC1
SEC1
UBP1
CES1
Cytosol
Mitochondria
AARDH
FAH
HPD
BHMT2
HGD
Amino acid metabolic process (Glycine, serine and threonine)
Pyruvate
CPS1
IDH1
MDH1
GLUD2
GLUD1
ALT1
AGXT
Citrate
Citrate Cycle
Urea Cycle
Argino succinate
ASS1
ASL
L-Alanine
AST2
AST1
α-ketoglutarate
AdoMet
MAT1A
GNMT
Methionine Cycle
Met
AdoHcy
DMG
BHMT
Hcy
Betaine
APOE
AKR1D1
Steroid metabolic process
ADH4
HMGCS2
ADH1A
ALDH1A1
CAT
Oxidative stress

"for TOC only"

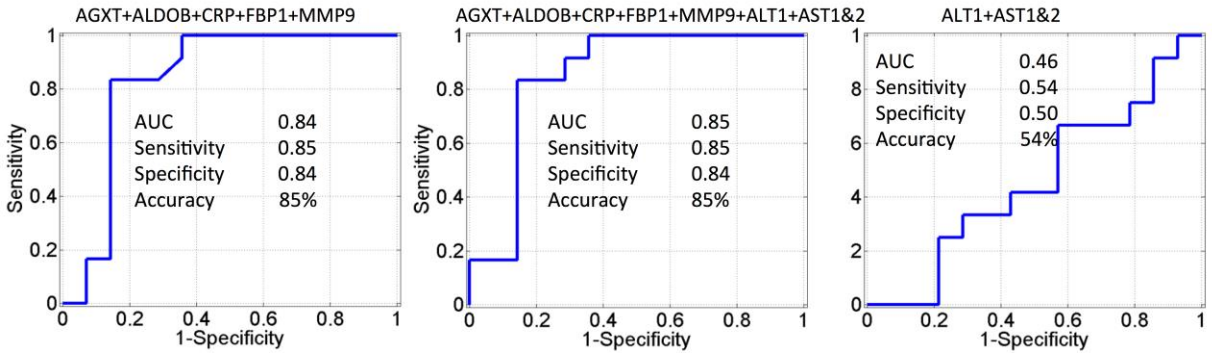
AGXT+ALDOB+CRP+FBP1+MMP9
AUC 0.84
Sensitivity 0.85
Specificity 0.84
Accuracy 85%
Sensitivity
1-Specificity
AGXT+ALDOB+CRP+FBP1+MMP9+ALT1+AST1&2
AUC 0.85
Sensitivity 0.85
Specificity 0.84
Accuracy 85%
Sensitivity
1-Specificity
ALT1+AST1&2
AUC 0.46
Sensitivity 0.54
Specificity 0.50
Accuracy 54%
1-Specificity